



Published in final edited form as:

Arch Ophthalmol. 2006 June ; 124(6): 853–859.

Visual Field Defects and Retinal Ganglion Cell Losses in Human Glaucoma Patients

Ronald S. Harwerth, PhD and

College of Optometry, University of Houston, Houston, Texas

Harry A. Quigley, MD

Wilmer Eye Institute, Johns Hopkins University, Baltimore, Maryland

Abstract

Objective—The depth of visual field defects are correlated with retinal ganglion cell densities in experimental glaucoma. This study was to determine whether a similar structure-function relationship holds for human glaucoma.

Methods—The study was based on retinal ganglion cell densities and visual thresholds of patients with documented glaucoma (Kerrigan-Baumrind, et al.) The data were analyzed by a model that predicted ganglion cell densities from standard clinical perimetry, which were then compared to histologic cell counts.

Results—The model, without free parameters, produced accurate and relatively precise quantification of ganglion cell densities associated with visual field defects. For 437 sets of data, the unity correlation for predicted vs. measured cell densities had a coefficient of determination of 0.39. The mean absolute deviation of the predicted vs. measured values was 2.59 dB, the mean and SD of the distribution of residual errors of prediction was -0.26 ± 3.22 dB.

Conclusions—Visual field defects by standard clinical perimetry are proportional to neural losses caused by glaucoma.

Clinical Relevance—The evidence for quantitative structure-function relationships provides a scientific basis of interpreting glaucomatous neuropathy from visual thresholds and supports the application of standard perimetry to establish the stage of the disease.

Keywords

Glaucoma; retinal ganglion cells; perimetry; clinical patients

Introduction

Glaucoma is a disease that causes a progressive loss of vision from the death of retinal ganglion cells^{1,2} and, it is reasonable that the degree of vision loss would be proportional to the amount of ganglion cell loss.³⁻⁹ Traditionally, this relationship between structure and function in glaucoma has been applied in clinical perimetry to establish the clinical stage, or severity, of the disease,¹⁰⁻¹⁵ but the quantitative relationship between visual sensitivity and ganglion cell density was established only recently.¹⁶ The quantitative structure-function model, which was developed from data on experimental glaucoma in monkeys, was accurate and relatively precise in predicting the retinal ganglion cell density underlying a given sensitivity and location in the visual field. Although based on experimental glaucoma, the model should be applicable

to clinical glaucoma because the visual systems of humans and monkeys are essentially identical.¹⁷⁻¹⁹ However, direct empirical evidence of the structure-function relation for clinical glaucoma is an important verification of the scientific basis of interpreting glaucomatous optic neuropathy from visual thresholds.

Previous investigations of ganglion cell density and visual sensitivity for human glaucoma patients have suggested a highly variable relationship.^{6,8} For example, in a recent study with a relatively large number of glaucoma patients, Kerrigan-Baumrind, et al.⁸ reported that linear regression analysis of the point-wise correlation between visual sensitivity and ganglion cell loss accounted for only 3% of the total variance. A clearer relationship between neural and visual losses was established by their finding that statistically significant visual field abnormalities occurred if neural losses at the corresponding retinal location exceeded 25 – 35%. In addition, the relationships between structure and function were highly significant with more global measures of visual sensitivity and neural loss, e.g., average visual sensitivity losses or the Mean Deviation (MD) perimetry indices vs. mean ganglion cell losses. Thus, although the study demonstrated a clinically significant structure-function relationship, it was not as quantitative for the point-wise translation of clinical measurements by perimetry to retinal ganglion cell losses as was found for experimental glaucoma. There are several possible explanations for the differences between the data for monkeys and humans, e.g., true species differences, variations in the pathophysiology of normal clinical glaucoma and experimental glaucoma, or post-mortem alterations in the human tissues. However, there were also differences in the methods of data analysis that may have affected the precision of estimating ganglion cell densities from perimetry data. Specifically, there were 1) differences in the data transformation for scaling visual sensitivities and neural cell densities and 2) retinal eccentricity was dealt with categorically for clinical glaucoma, rather than an independent parameter, as in the study of experimental glaucoma. Therefore, the purpose of the present investigation was to determine whether the relationships between ganglion cell density and visual sensitivity that were found for experimental glaucoma also hold for clinical glaucoma. Some of the results of these studies have been presented briefly elsewhere (Harwerth RS, Quigley HA. IOVS 2004;45:ARVO E-abstract 3473).

Materials and methods

The data for this study were the original data for retinal ganglion cell densities and visual thresholds at corresponding locations in the same eyes, which were published by Kerrigan-Baumrind, et al.⁸ The procedures for acquiring eyes and processing tissue have been described in detail in the published study and only the aspects that are relevant to the current analysis will be described.

The control data for normal retinal ganglion cell densities were from 17 eyes of 17 patients (mean age of 76.4 ± 11.0 years) without detectable ocular disorders that would affect retinal ganglion cells. The data from glaucoma patients were from 17 eyes from 13 patients (mean age of 72.2 ± 9.3 years). Each patient had a documented history of glaucoma with full-threshold visual field data obtained within the last two years of life. All of the clinical data were with an HFA-1 perimeter (Humphrey Field Analyzer, Carl-Zeiss Meditec, Dublin, CA) and no SITA fields were included. The characteristics of the individual glaucoma patients and the global indices from their perimetry data (if available) are presented in Table 1.

Histologic preservation of all of the eyes was achieved within 24 hours of death (usually within 12 hours) using aldehyde fixative. Tissue samples were collected for retinal areas that corresponded to 28 test field locations (illustrated in Fig. 1) for the HFA C24-2 program, using a conversion ratio of 1 mm retinal distance per 3.5 deg of visual angle. The actual number of samples per eye that were suitable for histology varied from 26 to 28 for the control eyes and

from 17 to 28 for the glaucomatous eyes (the number of samples for each glaucoma patient is presented in Table 1). The retinal tissue samples were sectioned (1 μm thickness) and stained (0.1% thionine) for histologic cell counts. The number of nuclei thought to represent retinal ganglion cells in the ganglion cell layer of each section, as well as the length of the section, was determined for 4 sections at each sample location. The data from the four sections were averaged to provide mean cells per unit length (ganglion cells/mm). For the present study, the original linear density data were converted to cell density per unit area (ganglion cells/mm²) for comparison to other published data and for application of the model. The cell densities were estimated by Ambergrombie's method for deriving densities from sectioned tissue,^{7,20,21} using the tissue section thickness of 1 μm and an average cell body diameter of 9 μm for the calculations. The cell densities were then transformed to a decibel (dB) scale by 10-times the logarithm of the calculated cell density for comparison of the corresponding HFA measurements of visual sensitivity. Thus, for example, a cell density of 10,000 cells/mm² is equal to 40 dB.

The structure-function model was developed to determine retinal ganglion cell densities at specific retinal locations from the corresponding HFA visual sensitivities. The specific details for the model have been described previously.¹⁶ In brief, the model was derived from the concept that visual thresholds represent a nonlinear pooling of the outputs of the neural detectors. The statistical properties of the pooling of neural responses should be independent of ganglion cell density, so that visual thresholds vary with the number of neural detectors when the number of detectors varies from retinal eccentricity, normal aging, or the stage of glaucoma.¹⁶

In agreement with others,²²⁻²⁶ the general expression between the neural density and visual sensitivity data was exponential and logarithmic transforms of both variables produced linear relationships for prediction of structural losses from functional measurements.¹⁶ However, the parameters of the linear function varied with eccentricity and, thus, the model required equations to determine the slope and y-intercept as a function of eccentricity, which in turn provided the parameters for the function for predicting ganglion cell density from visual sensitivity. The three equations are:

1. the slope of the function (m) at eccentricity (e): $m = (0.054 * e) + 0.95$
2. the intercept of the function (b) at eccentricity (e): $b = (-1.5 * e) - 14.8$
3. the predicted ganglion cell density (gc) for a sensitivity (s): $gc = (s - b) / m$

The application of the model for human glaucoma was evaluated by comparisons of the predicted ganglion cell densities as a function of the histologically measured ganglion cell densities. The predicted vs. measured cell densities were compared to a perfect one-to-one relationship and the goodness-of-fit was evaluated by three simple, intuitive statistics; 1) the coefficient of determination (r^2), 2) the mean absolute deviation (MAD), and 3) the distribution of residual errors (DRE). Each statistic evaluated a different property of the model. For example, r^2 as a measure of variability explained by the model was determined by the difference between the normal variation of predicted cell densities and the variation of predicted cell densities with respect to the unity function. The second statistic, the MAD is a measure of the mean error between the predicted and measured cell densities, without regard to the direction of error. The third evaluation of the goodness-of-fit, the DRE, is based on the signed errors, with errors of greater predicted than measured cell densities considered as negative errors and errors in the opposite direction considered as positive errors. The DRE is a useful analysis for densely clustered data to determine if the residual errors are systematic and as an assessment of the precision based on the 95% confidence limits of agreement between the model's predicted and measured values.

Results

The results of applying the model to data from glaucoma patients are shown in Figs. 2A & B. The upper graph (Fig. 2A) compares the ganglion cell densities predicted from perimetry measurements of visual sensitivity to the histological measurements of cell density. The different symbol shapes designate different locations in the visual field, as indicated by the sites of retina samples in Fig. 1. The data represent 437 sets of histologic measurements of from retinal locations with visual sensitivity greater than zero. The empirical data can be compared to the line of equality that is superimposed on the data, which by visual inspection appear to be scattered unsystematically around the line of unity correlation. The visual goodness-of-fit is verified by statistics for the coefficient of determination, indicating that the unity correlation accounts for 39% of the total variance, and by the MAD, indicating that the average error of the predicted ganglion cell density is less than 3 dB. Thus, the predicted one-to-one relationship for the structure-function model is only marginally worse than statistical linear regression ($m = 0.8$ dB/dB, $b = 8$ dB) which accounted for 42% of the variance.

The r^2 and MAD statistics demonstrate that the model is relatively accurate, but do not indicate the extent of systematic errors in the predicted values. In this respect, the DRE (Fig. 2B) demonstrates the errors are not systematic because the distribution is centered near zero with a standard deviation of 3.22 dB, and as shown by the three darker bars, about 65% of the data are within ± 3 dB of zero. The magnitudes of errors across the range ganglion cell densities are illustrated by the dashed lines in Fig. 2A that represent the 95% confidence limits for agreement between the predicted and measured values. Thus, the goodness-of-fit statistics indicate that, in the units of standard clinical measurements, the model is accurate and distribution of errors indicates that the model is relatively precise.

The full data set confirms a strong correlation between structure and function for the patients as a group, but it is also important to determine whether the model produces accurate results for individual patients. To illustrate the range of results, the data from the model for each patient-eye are listed in Table 1 and examples from six patients are presented in Fig. 3. The data listed in the table show that, for the majority of eyes, the model was quantitative with MAD's of < 3 dB for 12 of the 17 eyes and a mean of the DRE's < 2 dB for 11 of the 17 eyes, although the range of individual variation was large with r^2 values ranging from 0 to 0.71. With respect to individual examples, patients 10 and 5 (Figs. 3A & B) are the best examples of an accurate and precise relationship between predicted and measured ganglion cell densities. For both patients, the perimetry data were collected more than a year before the tissue samples and patient 10 had more advanced disease than patient 5 (MD = -9.10 dB and -4.75 dB, respectively). The data for these two patients are distinguished by the goodness-of-fit statistics (listed in Table 1) showing that the relationships for these individuals are more accurate and precise than for the group data. In contrast, the data for patients 15 and 12 (Figs. 3C & D) have systematic errors and the variance of the data with respect to the model is larger than the basic variance of the predicted cell densities. Because none of the variance can be explained by the model, the coefficient of determination for the model is zero (see Table 1). The errors for patients 15 and 12 are in opposite directions and are inconsistent with a simple explanation based on the time between the perimetry data and the death of the patient. On the other hand, these two patients may only represent a chance occurrence from random errors across, and within, patients, because the majority of patients are more consistent with the examples from patients 11 and 17 (Figs. 3E & F), in which the goodness-of-fit for an individual is similar to the group data. In addition, these two patients further illustrate that the degree of correlation does not depend on the stage of the disease. Thus, these results imply that there is a relatively accurate relationship between structure and function from clinical perimetry and, most likely, the precision is limited by nonsystematic variations within and across individuals.

The sources of variability in these data are unknown, but it may be that much of the imprecision is due to experimental error, rather than in the basic structure–function relationship or the model. This suggestion is based on a comparison of the data for clinical glaucoma and experimental glaucoma. The precision of clinical data is affected by aged patients who might be less motivated field-takers, by the normal aging effects on the state of the retinal tissue, and by the time delay between the visual fields and the tissue collection. With experimental glaucoma, the subjects are highly competent field-takers, with young eyes and immediate tissue processing. The effect of reducing these sources of error is demonstrated by comparison of data from humans and monkeys (Fig. 3). Figs. 2C & D present the results from experimental glaucoma, using the same model of structure–function relationships as for human patients (Figs. 2A & B). The statistical data for the model show a considerably greater precision in the relationship for experimental than clinical glaucoma, with an r^2 value of 0.85, compared to 0.39 for clinical glaucoma, and a narrower error distribution with about 75% of the data, compared to 65% for clinical glaucoma, falling within ± 3 dB of zero error. This comparison shows that when experimental variables are better controlled, the structure–function relationship becomes more precise. Thus, the overall results of the study confirm the fundamental assumption of clinical perimetry that the degree of vision loss is representative of the amount of ganglion cell loss.

Discussion

The most important outcome of the present study was to demonstrate a quantitative relationship between ganglion cell density and visual sensitivity for human clinical glaucoma. The data originally published by Kerrigan-Baumrind, et al⁸ were re-analyzed using a model that provided a point-by-point estimation of ganglion cell densities from perimetric measurements of visual sensitivities in corresponding retinal and test field locations.¹⁶ The model, without free parameters, produced an accurate and relatively precise quantification (in standard decibel units) of retinal ganglion cell densities associated with visual field defects eyes with glaucoma. The structure–function relationship for individual glaucoma patients was generally as good, or better, than for the grouped data.

The studies of structure–function relationships for clinical perimetry have demonstrated that two factors effectively reduce the variability of estimated neural losses, i.e., 1) logarithmic scaling of structure and function variables and 2) defining the parameters for the structure–function relationship by eccentricity. The significance of reduced variability, however, is most applicable for established visual field defects and the quantitative model does not improve the estimation of early neural losses using clinical perimetry. The detection of early neural losses by perimetry is constrained by inherent intersubject variation of psychophysical measures of normal thresholds. Because the relationship between the visual threshold and number of neural mechanisms is logarithmic, a relatively large proportion of ganglion cells (40 – 50%) must be lost before the threshold measurement exceeds the normal variability and reaches statistical significance. Therefore, these results do not contradict the previous reports that statistically significant visual field abnormalities occur only after 25 – 35% of ganglion cells have died⁸ or that the relationship between sensitivity and neural losses is systematic only after about 50% of the ganglion cells have died.⁷

The detection of early ganglion cell losses by perimetry might be improved by linearization of the structure and function data which, in comparison to the logarithmic scaling, will accentuate mild visual field defects and compress the range of defects associated with deep defects from advanced ganglion cell death.²⁷ Several investigators have proposed linear models to improve the accuracy of perimetry for early visual field defects,^{28,29} but when logarithmic and linear transformations were compared for correlating perimetric defects and neural losses from experimental glaucoma, it was found that the relationship in linear units was less systematic

in two respects.²⁷ First, the relationship exhibited considerable scatter in the data for small losses in visual sensitivity and, second, visual sensitivity losses became saturated with larger losses in ganglion cell density. Thus, although linear scaling of perimetric defects and ganglion cell losses potentially could improve the structure-function relationship for visual defects associated with small amounts of cell loss, the usefulness of the relationship is limited because of the high variability in that range. The comparatively greater variability with linear-loss functions is a likely consequence of the logarithmic scale of stimulus intensities for perimetry measurements and because the relationship between visual sensitivity and the number of neural detectors is nonlinear.

In conclusion, the study confirmed that visual field defects measured by standard clinical perimetry are a direct expression of the neural losses caused by glaucoma, where the quantitative relationship varies with retinal eccentricity. The eccentricity dependence of structure-function relationships is a consequence of the normal variation in ganglion cell density with retinal eccentricity while, at any given distance from fixation, the standard perimetric measures of visual sensitivities (dB units) provide an accurate estimation of ganglion cell densities in comparable decibel units. Although the present results suggested that the precision of estimates of ganglion cell densities may be somewhat lower for clinical than experimental glaucoma, it is likely that the apparent imprecision is related to difficulties in obtaining perimetry data and postmortem retinal tissue from patients rather than a difference in the fundamental structure-function relationship. In addition, for either experimental or clinical glaucoma, the precision of estimation is approximately equal across the entire range of ganglion cell loss, but logarithmic scaling of the relationship compresses small losses of both visual sensitivity and ganglion cell density and expands the ranges of larger losses.²⁷ Consequently, the accuracy and precision of the structure-function relationship is best for moderate to advanced glaucomatous neuropathy, which is the range where subjective measurements by perimetry are generally considered to be more accurate than objective structural measurements.³⁰⁻³⁵ It is for this reason that computer-automated perimetry has become, and is likely to remain, the “gold standard” for the assessment of the stage of neural damage from glaucoma.³⁶

Acknowledgements

These studies were supported by Alcon Research, Ltd. (Fort Worth, TX); Research grants EY01139 and EY02120, and Core Grants EY07551 and EY01765 from the National Eye Institute, the National Institutes of Health (Bethesda, MD), and by a John and Rebecca Moores Professorship from the University of Houston, Houston, TX.

References

1. Epstein, DL. Primary open angle glaucoma . In: Epstein, DL.; Allingham, RR.; Schuman, JS., editors. Chandler and Grant's Glaucoma. 4. Baltimore: Williams & Wilkins; 1997. p. 183-198.
2. Quigley HA. Neuronal death in glaucoma. *Progress in Retinal and Eye Research* 1999;18:39–57. [PubMed: 9920498]
3. Anderson, DR. Perimetry, With and Without Automation. second edition. Louis, St ; Mosby, CV.; Co, editors. 1987.
4. Alexander, LJ. Diagnosis and management of primary open-angle glaucoma. In: Classe, JG., editor. *Optometry Clinics Norwalk*. 1. Appleton & Lange; 1991. p. 19-102.
5. Quigley HA. Open-angle glaucoma. *The New England Journal of Medicine* 1993;328:1097–1106. [PubMed: 8455668]
6. Quigley HA, Dunkelberger GR, Green WR. Retinal ganglion cell atrophy correlated with automated perimetry in human eyes with glaucoma. *American Journal of Ophthalmology* 1989;107:453–464. [PubMed: 2712129]

7. Harwerth RS, Carter-Dawson L, Shen F, et al. Ganglion cell losses underlying visual field defects from glaucoma. *Investigative Ophthalmology and Visual Science* 1999;40:2242–2250. [PubMed: 10476789]
8. Kerrigan-Baumrind LA, Quigley HA, Pease ME, et al. Number of ganglion cells in glaucoma eyes compared with threshold visual field tests in the same persons. *Investigative Ophthalmology and Visual Science* 2000;41:741–748. [PubMed: 10711689]
9. Harwerth RS, Crawford ML, Frishman LJ, et al. Visual field defects and neural losses from experimental glaucoma. *Progress in Retina and Eye Research* 2002;21:91–125.
10. Hodapp, E.; Parrish, RKII.; Anderson, DR. *Clinical decisions in glaucoma*. St Louis, MO: Mosby - Year Book; 1993. p. 52-61.
11. Advanced Glaucoma Intervention Study. 2. Visual field test scoring and reliability. *Ophthalmology* 1994;101:1445–1455. [PubMed: 7741836]
12. Brusini P. Clinical use of a new method for visual field damage classification in glaucoma. *European Journal of Ophthalmology* 1996;6:402–407. [PubMed: 8997583]
13. Kass MA, Heuer DK, Higginbotham EJ, et al. The Ocular Hypertension Treatment Study: a randomized trial determines that topical ocular hypotensive medication delays or prevents the onset of primary open-angle glaucoma. *Archives of Ophthalmology* 2002;120:701–713. [PubMed: 12049574]
14. Heijl A, Leske MC, Bengtsson B, et al. Early Manifest Glaucoma Trial Group. Reduction of intraocular pressure and glaucoma progression: results from the Early Manifest Glaucoma Trial. *Archives of Ophthalmology* 2002;120:1268–1279. [PubMed: 12365904]
15. Budenz DL, Rhee P, Feuer WJ, et al. Comparison of glaucomatous visual field defects using standard full threshold and Swedish interactive threshold algorithms. *Archives of Ophthalmology* 2002;120:1136–1141. [PubMed: 12215086]
16. Harwerth RS, Carter-Dawson L, Smith ELIII. Neural losses correlated with visual losses in clinical perimetry. *Investigative Ophthalmology and Visual Science* 2004;45:3152–3160. [PubMed: 15326134]
17. Harwerth RS, Smith EL. Rhesus monkey as a model for normal vision of humans. *American Journal of Optometry and Physiological Optics* 1985;62:633–641. [PubMed: 4050966]
18. Boothe RG, Dobson V, Teller DY. Postnatal development of vision in human and nonhuman primates. *Annual Review of Neuroscience* 1985;8:495–545.
19. Harwerth RS, Smith EL, DeSantis L. Behavioral perimetry in monkeys. *Investigative Ophthalmology and Visual Science* 1993;34:31–40.
20. Ambercrombe M. Estimation of nuclear population from microtome sections. *Anatomical Record* 1946;94:239–247.
21. Wassle H, Grunert U, Rohrenbeck J, et al. Retinal ganglion cell density and cortical magnification factor in the primate. *Vision Research* 1990;30:1897–1911. [PubMed: 2288097]
22. Pirenne MH. Binocular and monocular thresholds for vision. *Nature* 1943;153:698–699.
23. Nachmias J. On the psychometric function for contrast detection. *Vision Research* 1981;21:215–223. [PubMed: 7269298]
24. Robson JG, Graham N. Probability summation and regional variation in contrast sensitivity across the visual field. *Vision Research* 1981;21:409–418. [PubMed: 7269319]
25. Tolhurst DJ, Movshon JA, Dean AM. The statistical reliability of signals in single neurons in cat and monkey visual cortex. *Vision Research* 1983;23:775–785. [PubMed: 6623937]
26. Harwerth, RS.; Smith, EL. The intrinsic noise of contrast sensitivity perimetry. In: Wall, M.; Wild, J., editors. *Perimetry Update 2000/2001*. The Hague, The Netherlands: Kugler Publications; 2001. p. 59-68.
27. Harwerth RS, Carter-Dawson L, Smith EL, et al. Scaling the structure-function relationship for clinical perimetry. *Acta Ophthalmologica Scandinavia* 2005;83:448–455.
28. Garway-Heath DF, Capriolo J, Fitzke FW, et al. Scaling the hill of vision: the physiological relationship between light sensitivity and ganglion cell numbers. *Investigative Ophthalmology and Visual Science* 2000;41:1774–1782. [PubMed: 10845598]

29. Swanson WH, Feliuss J, Pan F. Perimetric defects and ganglion cell damage: interpreting linear relations using a two-stage neural model. *Investigative Ophthalmology and Visual Science* 2004;45:466–472. [PubMed: 14744886]
30. Drance SM. Doyne Memorial Lecture, Correlation of optic nerve and visual field defects in simple glaucoma. *Transactions Ophthalmological Society UK* 1975;95:288–296.
31. Sommer A, Katz J, Quigley HA, et al. Clinically detectable nerve fiber atrophy precedes the onset of glaucomatous field loss. *Archives of Ophthalmology* 1991;109:77–83. [PubMed: 1987954]
32. Sanchez-Galeana C, Bowd C, Blumenthal EZ, et al. Using optical imaging summary data to detect glaucoma. *Ophthalmology* 2001;108:1812–1818. [PubMed: 11581054]
33. Greaney MJ, Hoffman DC, Garway-Heath DF, et al. Comparison of optic nerve imaging methods to distinguish normal eyes from those with glaucoma. *Investigative Ophthalmology and Visual Science* 2002;43:140–145. [PubMed: 11773024]
34. Johnson CA, Sample PA, Zangwill LM, et al. Structure and function evaluation (SAFE): II Comparison of optic disk and visual field characteristics. *American Journal of Ophthalmology* 2003;135:148–154. [PubMed: 12566017]
35. Matsumoto C, Shirato S, Haneda M, et al. Study of retinal nerve fiber layer thickness within normal hemivisual field in primary open-angle glaucoma and normal-tension glaucoma. *Japanese Journal of Ophthalmology* 2003;47:22–27. [PubMed: 12586174]
36. Johnson CA. Standardizing the measurement of visual fields for clinical research. *Ophthalmology* 1996;103:186–189. [PubMed: 8628553]

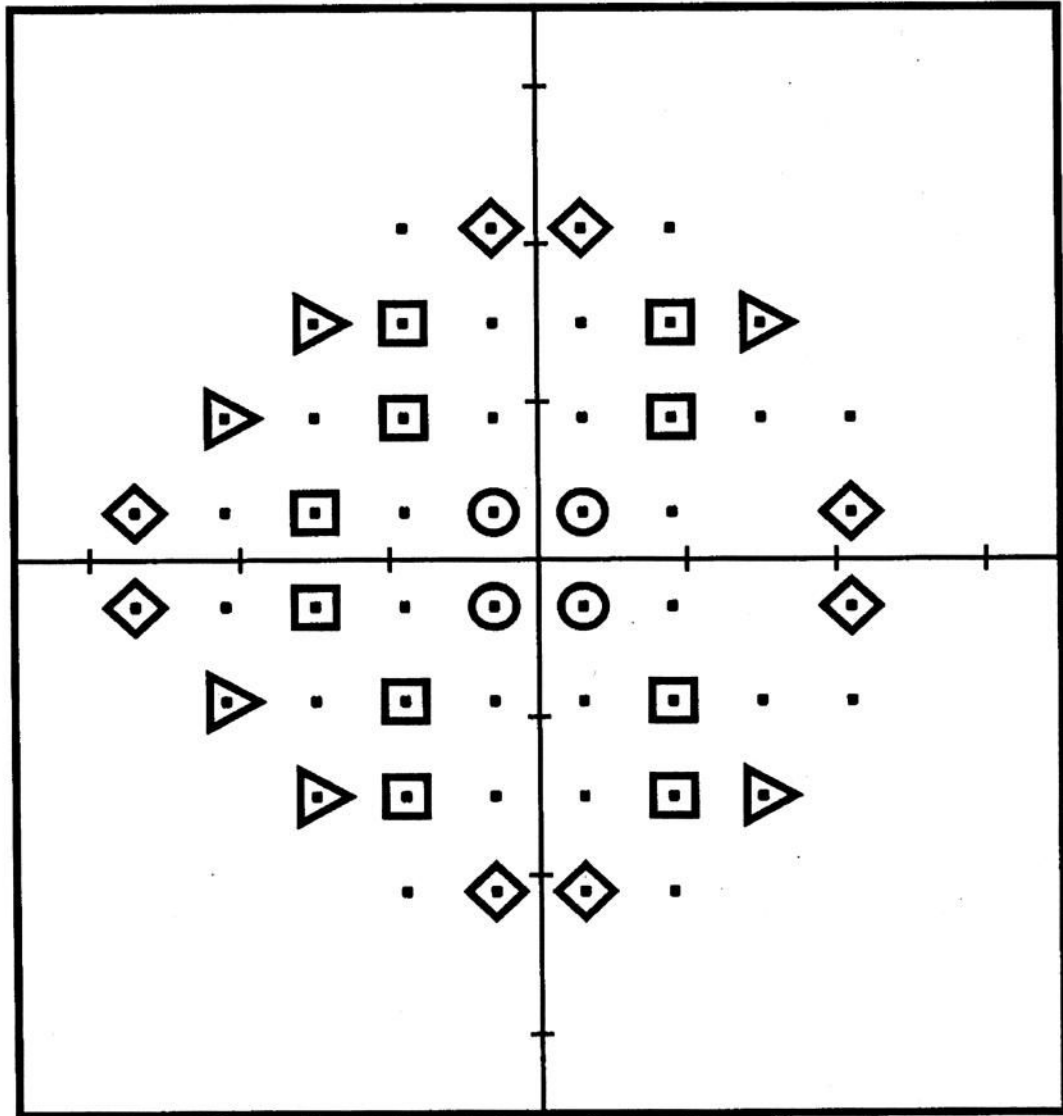


Fig. 1. Test field locations from the Humphrey Field Analyzer C24-2 program (Carl-Zeiss Meditec, Dublin, Calif) that corresponded to retinal locations of the tissue samples for histologic cell counts. The symbols represent the 28 sites that were used for the correlation of retinal ganglion cell density and visual field sensitivity in eyes of patients with glaucoma. The symbol shapes that are used to designate visual field locations for retinal tissue samples are also used in Figures 2 and 3 to represent the visual field and retinal locations of the data for comparing the predicted and measured ganglion cell density.

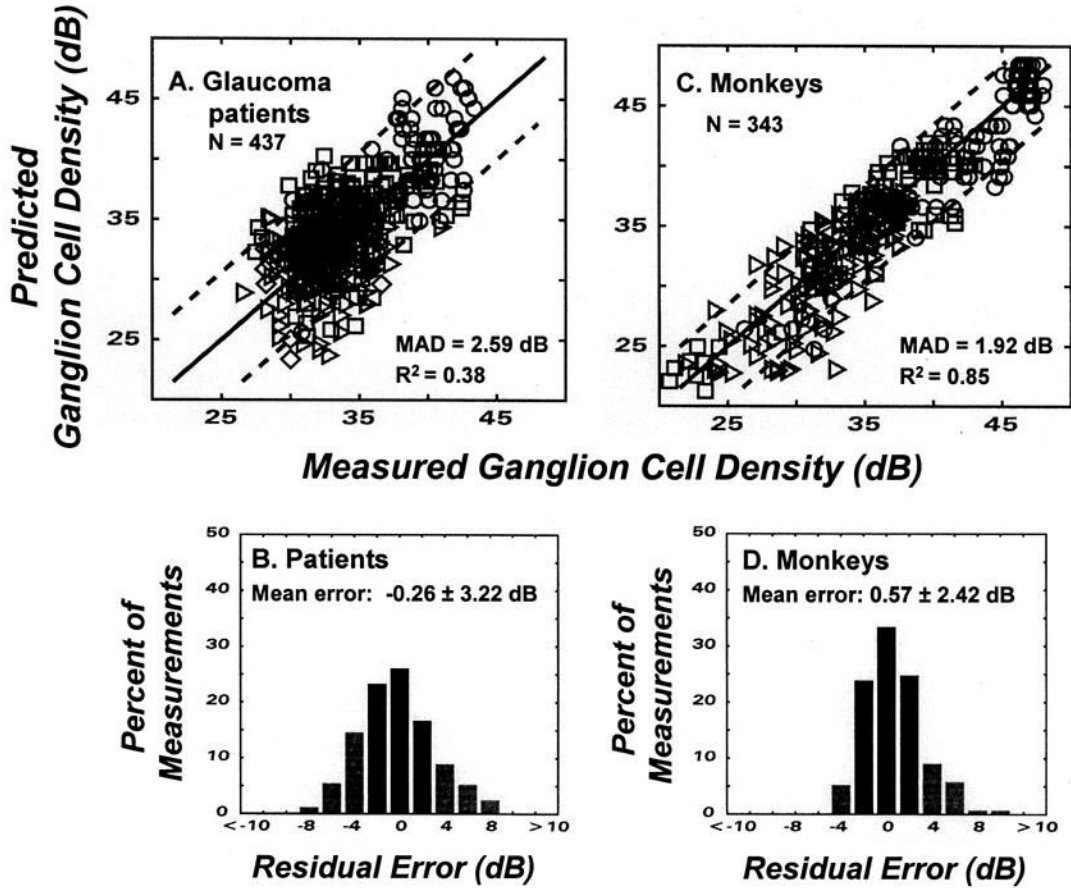


Fig. 2. The application of the model for structure-function to glaucoma patients and monkeys with experimental glaucoma. The upper graphs (**A & C**) represent the relationships between ganglion cell densities predicted from perimetry measurements of visual sensitivity as a function of the histological measurements of cell density. The different symbol shapes designate different locations in the visual field, as indicated by the sites of retina samples in Fig. 1. The model prediction of unity correlation is shown by the one-to-one line that is superimposed on the data. Goodness-of-fit statistics for the mean absolute deviation (MAD) and coefficient of determination (r^2) are presented as insets and the limits of agreement (95% confidence limits) are illustrated by the dashed lines on each graph. The lower histograms (**B & D**) present the distribution of residual errors (DRE) of the model with respect to the one-to-one relationship, with errors of greater predicted than measured cell densities designated as negative errors and errors for greater measured than predicted cell densities designated as positive errors. The mean and SD's of the distributions are shown by insets and the percentage of errors that are less than ± 3 dB are indicated by the darker bars.

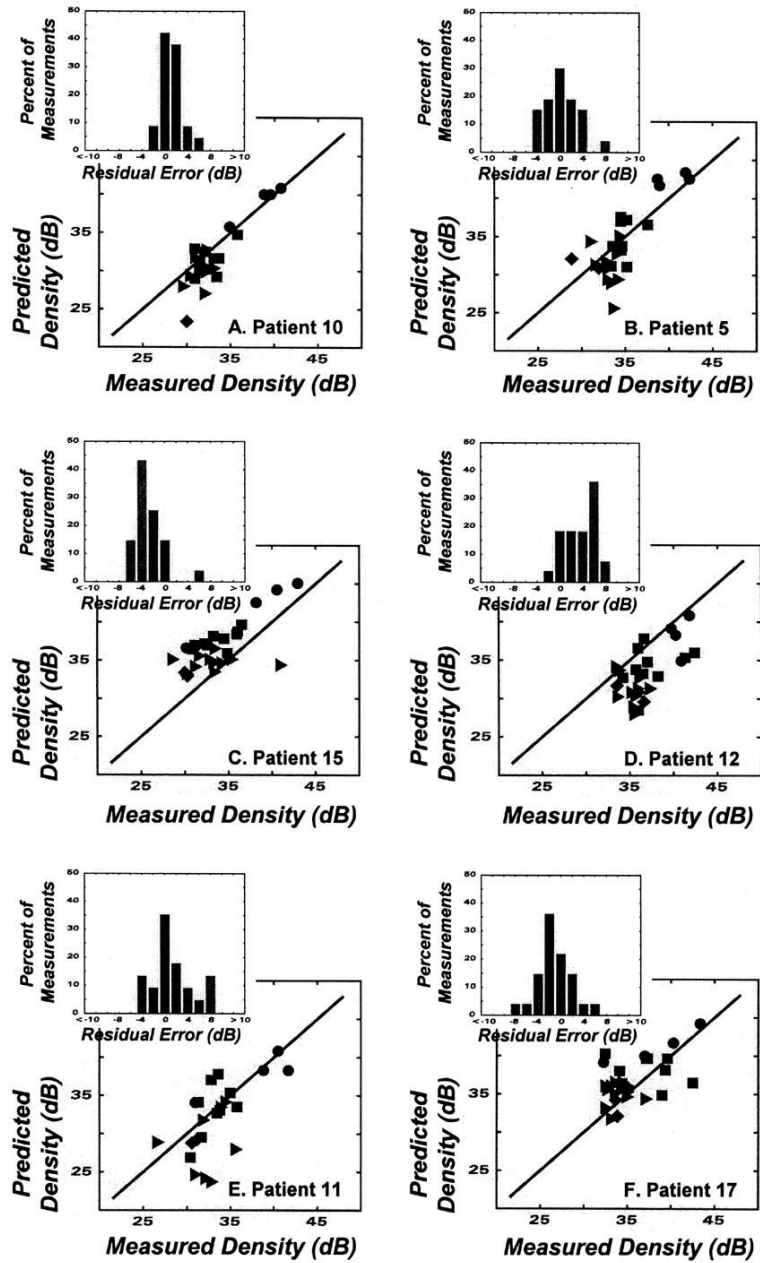


Fig. 3. Results after applying the model for structure-function to the data for individual eyes in patients with glaucoma. Details of the data are the same as for the group data in Figure 3, and details of patients and model results are given in the Table.

Table 1
 Characteristics of patients and data from the structure-function model

Patient - eye #	Patient Data		HFA Global Indices		Number of samples	Model Data		
	Age (years)	TBD (days)	MD (dB)	PSD (dB)		r^2	MAD (dB)	MRE \pm sd (dB)
1	87	84	-4.85	4.56	27	0.33	2.21	-1.82 \pm 2.06
2	81	87	-3.09	2.19	28	0.05	3.10	-2.69 \pm 2.22
3	83	408	-6.03	2.27	28	0.12	1.88	-1.43 \pm 1.66
4	75	339	-15.60	14.31	17	0.22	3.71	-2.88 \pm 3.35
5	77	515	-4.75	NA	27	0.65	2.31	0.36 \pm 2.91
6 ^{&}	78	202	-13.19	10.12	19	0.65	2.44	1.00 \pm 2.97
7	62	368	-6.44	9.58	23	0.07	2.62	-0.40 \pm 3.37
8 [@]	62	712	-5.28	2.72	28	0.24	2.14	0.99 \pm 2.39
9	73	151	-10.84	6.95	27	0.08	3.52	2.88 \pm 3.04
10 ⁺	70	458	-9.10	4.43	24	0.67	1.70	1.14 \pm 2.03
11 ^{&}	78	202	-9.22	NA	23	0.33	2.85	1.32 \pm 3.68
12 [@]	62	712	-6.96	3.53	28	0	3.77	3.58 \pm 2.65
13 ⁺	70	2000	-7.33	5.05	27	0.71	1.48	0.52 \pm 1.90
14	74	319	0.78	2.72	28	0.39	2.15	-0.74 \pm 2.71
15	67	125	-7.33	NA	28	0	3.29	-2.82 \pm 2.59
16 [#]	52	375	NA	NA	27	0.34	2.61	-2.26 \pm 2.07
17 [#]	52	375	NA	NA	28	0.20	2.47	-1.23 \pm 2.91

Abbreviations: TBD – Time Before Death for the collection of perimetry data, HFA – Humphrey Field Analyzer, MD – Mean Deviation, PSD – Pattern Standard Deviation, dB – decibels, r^2 – coefficient of determination, MAD – Mean Absolute Deviation, MRE – Mean Residual Error, sd – Standard Deviation, NA – not available, Patients – eyes with the same superscript symbols indicate pairs of eyes from the same patient.